International Journal of Applied Engineering Research ISSN 0973-4562 Volume 12, Number 4 (2017) pp. 470-481

Effect of corrugated web on flexural capacity of steel beams

Ahmed S. Elamary[*1,3], Amr B. Saddek[2] and Mamdooh Alwetaishi[3]

[1]*Civil Engineering Department, Al-Azhar University, Qena, Egypt.*

[2]*Civil Engineering Department, Beni-Suef University, Egypt*

[3]*Civil Engineering Department, College of Engineering, Taif University, Saudi Arabia*

Abstract:

Flexural strength evaluation is important in the design of steel beams. In the current work, experimental and analytical study has been carried to define flexural capacity of conventional steel I beams and steel beam with corrugated web (CW). Full-scale steel beam with flat web (FW) or CW has been tested to verify the flexural behavior of each beam type. The experimental program was conducted for four simply supported beams with different web configurations (Flat or Corrugated) and different flange compactness (non-compact or compact). Experimental work has defined the reduction effect due to corrugated web on flexural capacity of steel beam. Nonlinear finite element technique was used to model the tested specimens and verified experimental work results. The experimental program was extended to study the effect of CW on flexural behavior of composite concrete-steel beam. Two additional composite concrete-steel beams with corrugated web have been fabricated and tested under flexural loads. The composite beams test results have been compared with the nominal moment capacity (NMC) for the composite beam. The NMC has been obtained by using a limit state design process taking into consideration the effect of CW in flexural behavior obtained previously for bare steel beams. The comparison between the designed values of bending moment agreed to an acceptable degree of accuracy with the values obtained experimentally.

Keywords: Corrugated webs, Flexural capacity, Steel beams, Flange compactness

INTRODUCTION

Many studies on the flexural behavior of steel beams with CWs have been carried out, Abbas (2003), Huang et al. (2004), Egaaly et al. (1997), Khalid et al. (2004), Oh et al. (2012) conducted experiments, finite element and theoretical analysis on the accordion effect of steel beams with CWs. Furthermore, there is no interaction between flexure and shear behaviors of these girders. Thus, the ultimate moment capacity of a steel girder with a corrugated steel web can be based on the flange yield strength (Leiva-Aravena, 1987; Protte, 1993; Elgaaly et al., 1997; Johnson and Cafolla, 1997; Sayed-Ahmed, 2007). The flexural capacity of composite girders with corrugated steel webs was also investigated and the same aspects defined for steel girders were found to be applicable to composite girders (Metwally and Loov, 2003). Lindner (1992), Aschinger and Lindner (1997) studied the elastic flexural behavior of CW I-girders under in-plane loads. In their analyses, they assumed that the flanges carry only the moment and the web carries only the shear. Elgaaly et al. (1997) carried out experimental and analytical studies on bending strength of steel beams with CWs. Parametric analytical studies were performed to examine the effect of the ratio between the thicknesses of flange and web, the corrugation configuration, the panel aspect ratio, and the stress-strain relationship to the ultimate bending moment capacity of steel beams with CWs. Chan et al. (2002), Khalid et al. (2004) studied the influence of web corrugation on the bending capacity of the beam using finite element method. Beams with FW, horizontally CW and vertically CW were studied. Watanabe and Kubo (2006) presented test and numerical analysis results of CW girders with four different trapezoidal corrugation configurations under pure bending. A predicting method of the ultimate strength considering local flange buckling was also proposed based on the parametric analysis of CW girders.

However, CW beams have some weaknesses due to geometric characteristics. First, the local buckling strength of the flange can be smaller than that of FW beams, because the largest outstand of a flange in CW beams is larger than that of FW beams (Pasternak and Kubieniec, 2010). Second, as a result of web eccentricity, additional in-plane transversal moment occurs in flanges (Abbas et al., 2006). This moment reduces the flexural strength of CW beams. Third, only flanges, except for the web, contribute to the flexural strength of CW beams, due to the accordion effect of CWs (Elgaaly et al., 1997). Various significant results were achieved by the mentioned studies. However, a considerable uncertainty still exists regarding the a certain value which reflect the effect of using CW instead of FW on the flexural capacity of steel I beams. Therefore, an experimental study on the effects of CW on the flexural failure mechanism expected to occur in steel beams presented in this paper. Accordingly, four

specimens with different steel flange compactness factor and web configuration FW or CW were fabricated and tested. Each specimen contain the central panel which subjected to pure moment as well as stiffened steel beams with flat panels adjacent to the support were employed in this experimental study. The four steel beams, divided into two groups based on web shape, two beams each. The difference between the two groups was as follows: web configuration and flange compactness. The first group consists of two beam with CW where the flange compactness was different. The second group consists of two beams with FW and different flange compactness factor. All specimens were tested under four-point bending with loading at one-third span points, resulting in zero shear and a constant moment in the middle one-third of the span. The experimental program extend to verify the results obtained from the first part of the experimental program in the composite concrete-steel beam with corrugated web test using the same test procedure applied for the bare steel beams.

EXPERIMENTAL PROGRAM

Test specimens

Fabrication of specimens

To identify the flexural behavior and strength of steel beam with FW and compare its behavior with beams have similar properties and dimensions but with CW, full-scale FW or CW beams were tested under four points load. The tested Beams had 1850 mm approximate length with an effective span of 1750 mm. The beams consist of two stiffened panels and central slender panel. The FW or CW was connected to the flanges from one side only, with continuous 4 mm fillet welds, using gas metal arc welding. The size of weld for connecting built up section and end connecting plates was taken according to the Egyptian Code of Practice for Steel Construction and Bridges No. 205. Careful procedures of welding were followed to avoid distortion of the beam result from the high temperature from welding process especially for slender parts. The parameters in the specimens were flange thicknesses (t_f = 4, 10 mm), and web shape (flat or corrugated) with 2.1mm thickness. The corrugation profile of the specimens is shown in Figure 1. The length of the horizontal panel, b, was 100 mm, the length of the corrugation depth, h_r, was 50 mm, and the projected length of the inclined panel, d, was 50 mm. The corrugation angle, θ, was 45°. The height of the CW, h_w, and thickness of CW, t_w, the width of the flange, b_f , and thickness of the flange, t_f , and the ratio of height to thickness of the CW, h_w/t_w, yield stress of the flange and the web, F_{yf} and F_{yw}, and the web slenderness ratio, λ_p , of specimens are summarized in table 1.

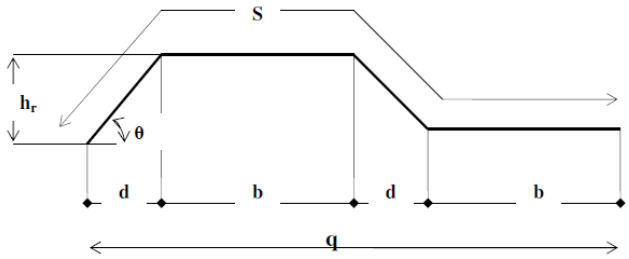

Figure 1: details of corrugation profile

Table 1: Average dimensions of cross-section

Average dimension of cross Sections and width-to-thickness ratios of specimens							
Specimen No.	h (mm)	t_w (mm)	b_f (mm)	t_f (mm)	h/t_w	C/t_f	Flange Compactness Classification
CWNCF101	400	2.1	100	4	200	18.75	Slender
CWCF102	400	2.1	100	10	200	7.5	Compact
FWNCF201	400	2.1	100	4	200	12.5	Non-compact
FWCF202	400	2.1	100	10	200	5	Compact

Test setup

The specimens tested under two lines loading, as shown in Fig. 2. A concentrated load from the actuator was distributed by the transfer beam. The capacity of the actuator was 1,000 kN. The central region with FW or CW, L (=0.4 m), was subjected to constant bending moment. In both sides of the central region, L1 (=0.75 m), the FW of 12 mm plates with vertical and horizontal stiffeners was used to prevent shear buckling. To prevent sudden lateral movement and torsion of specimens, lateral supports were installed leaving 2 mm spacing between the specimen and lateral supports. The lateral supports were spaced 1.60 m apart away from the transfer beam. The unbraced length of compressive flanges of specimens was 1.60 m, by the locations of lateral supports. To measure the strain of specimens, strain gauges were attached to the webs, as shown in Fig. 2(b). Linear variable displacement transformers (LVDT) were installed to measure two kinds of displacements of specimens; the vertical

deflections, and the out-of-plane displacements of the CWs. To measure the vertical deflections of the specimens, LVDT was installed at the location in mid-span of the central region, as illustrated in Fig. 2(b). To measure the out-of plane displacement of the webs, LVDTs were installed at the location in mid-span of the central region shown in Fig. 2(b).

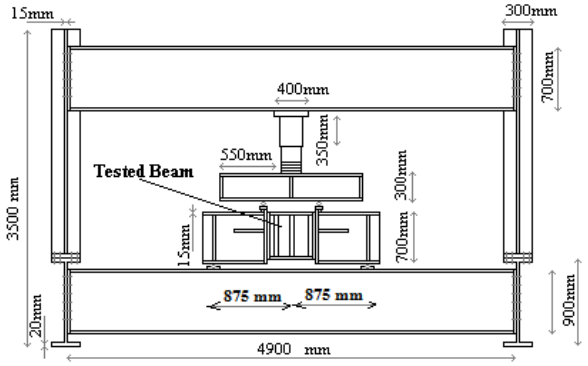

a- Test setup

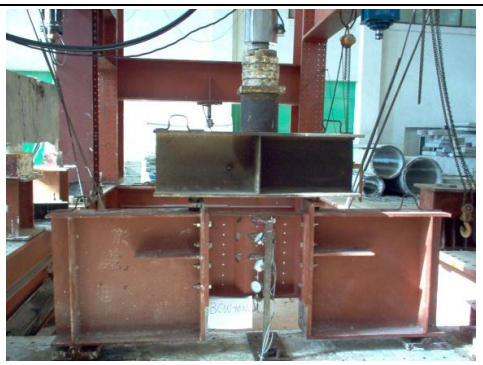

b- Specimen under test

Figure 2: Test setup and specimen under test

Materials

Coupon test

To determine the mechanical properties of the steel used in this experimental work, three standard tension coupons were cut from each specimen; the first from the compression flange, the second from tension flange and the third from the web. The coupons were cut as far as possible from the flame cut side and machined to the nearest 0.01mm. The coupons were prepared and tested according The stress strain curve was obtained and plotted as shown in Fig.3. The results such as modulus of elasticity, elongation percentage, ultimate and yield stresses obtained from these tests are listed in Table 2. Tensile coupon test was conducted in accordance with to the Egyptians Standard Codes No 76 for Tensile Test of Metals, having a gauge length of 160 mm (including embedded distance of each jaw of the testing machine). The tension coupons were tested in a 500 kN capacity displacement controlled testing machine using friction grips to apply the loading.. The average yield stresses of the flange and the web materials from coupon tests are summarized in Table 2. The average yield stress of the flange material of 10 mm thick, F_{yf} , was 280MPa. The average yield stress of the CW material (F_{yw}) of 2.1 was 310MPa. Figure 3 plots the stress-strain curves from 2.1coupons used in webs. These coupons yielded at the strain of 0.0014. Based on test results, the yield strain of these plates, ε_y, was assumed to be equal to 0.0014

.

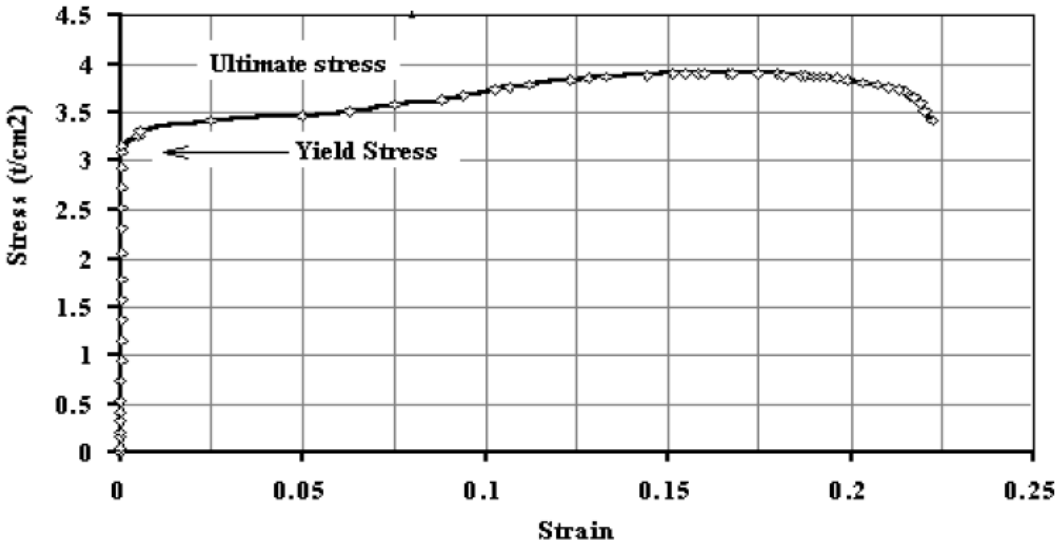

Figure 3: Tensile test results for web coupon

Table 2: Modulus of Elasticity, Elongation percentage, Ultimate and Yield stresses

Coupon Type	F_Y (N/mm^2)	F_u (N/mm^2)	E (N/mm^2)	δ %
Compact Flange	300	375	200000	28
Non-compact Flange	320	390	213000	25
Web	310	390	205000	24

Failure mechanism

Specimens CWNCF101 and FWNCF201 after failure are shown in figure 4; the vertical flange buckling into the corrugated and FW beams can be noted in these specimens. The flange and the CW buckled abruptly at the mid span of the specimen, after yield of the top flange. As the load increased, the buckling in the top flange increased, and then the local buckling started to be deformed in case of FW only. During the test, the strength of the bottom flange degraded, and made the bottom flange yield first before the top flange yielded.Until the bottom flange yielded, the specimen behaved elastically, showing a linear relationship of load-displacement curves. After the bottom flange began to yield, the bending stiffness of the specimen gradually decreased. After the whole section of the bottom flange yielded, and the top flange began to yield, the bending stiffness of the specimen considerably decreased. Unlike the steel beam with the FW, the steel beam with CW behavior did not show any local web buckling.

Specimens CWCF102 and FWCF202 after failure are shown in figure 5; the top flange behave as compact flange during all test time and without local buckling. The FW buckled abruptly at the mid span of the specimen in the top middle part. As the load increased, the buckling in the local web buckling increased till failure. The behavior of steel beam with CF and CW was controlled by the global web buckling.

a- Failure shape of steel beam with CW.

b- Failure shape of steel beam with FW.

Figure 4: Steel beam specimens with non-compact flanges after testing

a) Failure shape of steel beam with CW

b) Failure shape of steel beam with FW.

Figure 5: Steel beam specimens with compact flanges after testing

Test results

Figure 6 shows mid span vertical displacement of test specimens according to the applied vertical load obtained experimentally. In table 3, the maximum load achieved by each specimen with the crossponding maximum displacement were listed. From these values it can be conclude that the flexural strength of steel beams could be decreased from 10% to 20% in case of using corrugated web instead of flat web.

Table 3: Maximum load and displacement obtained experimentally

Spec. No.	Max. load (kN)	Max. displacement (mm)	Load (%) from reference	**Note**
CWNCF101	100	12	80	
CWCF102	345	13	87	
FWNCF201	125	4.2	1	reference
FWCF202	400	10	1	reference

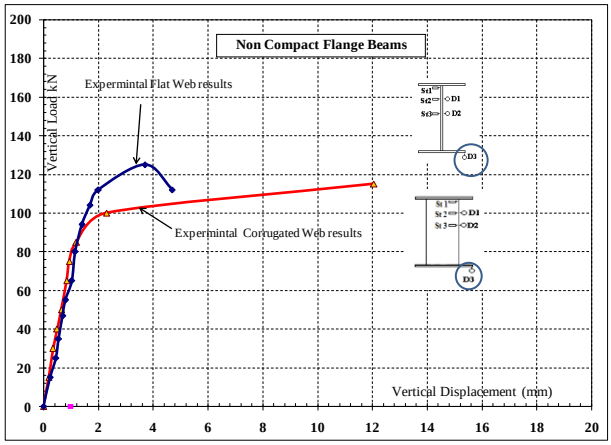

a. Beams with non-compact flanges and CW or FW

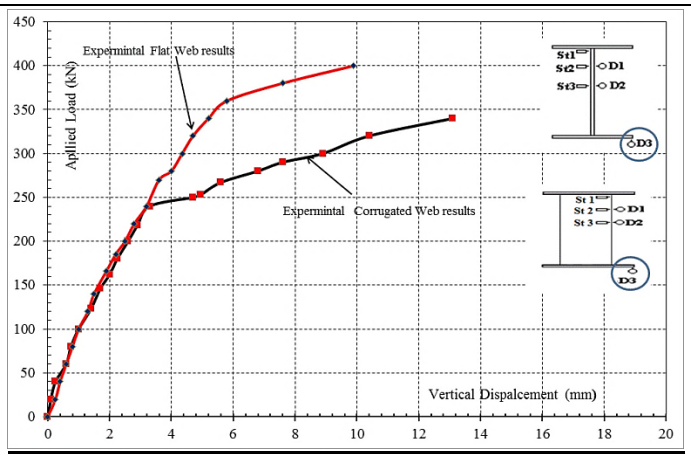

b. Beams with compact flanges and CW or FW

Figure 6: Load vs mid-span deflection - Experimental results of bare Steel beams

FINITE ELEMENT MODELING

The finite element elastic-plastic shell (Shell43) was considered for steel section which built in ANSYS software package. The element Shell43 is defined by four nodes having six degrees of freedom at each node. The deformation shapes are linear in both in-plane directions. The Shell43 element is capable of describing plasticity, large deflections and large strains. The element allows for plasticity, creep, stress stiffening, large deflections, and large strain capabilities. In order to avoid numerical problems, the values measured in the experimental tests for the material properties of the steel components (webs and flanges) were used in the finite element analyses. Displacement boundary conditions were needed to constrain the model to get a unique solution. To ensure that the model acts in the same way as the experimental beam boundary conditions need to be applied at the supports and loadings exist. The support was modeled in such a way that hinged and roller were created. A single line of nodes on the plate were given constraint in the Y, and X directions, applied as constant values of zero in one side , where in the other side a single line of nodes on the plate were given constraint in the X only. The force applied at ten nodes each node on the plate is one tenth of the actual force applied to eliminate the effect of located strain in each node. Figure 1 illustrates the applied loads and boundary condition for meshed steel beam with flat or CW. The finite element mesh in the models was investigated by varying the size of elements. In the flanges and web, the size of the elements was 25 mm (length and width). The typical finite element models of steel beams with corrugated or FW subjected to vertical loads are shown in Fig. 7.

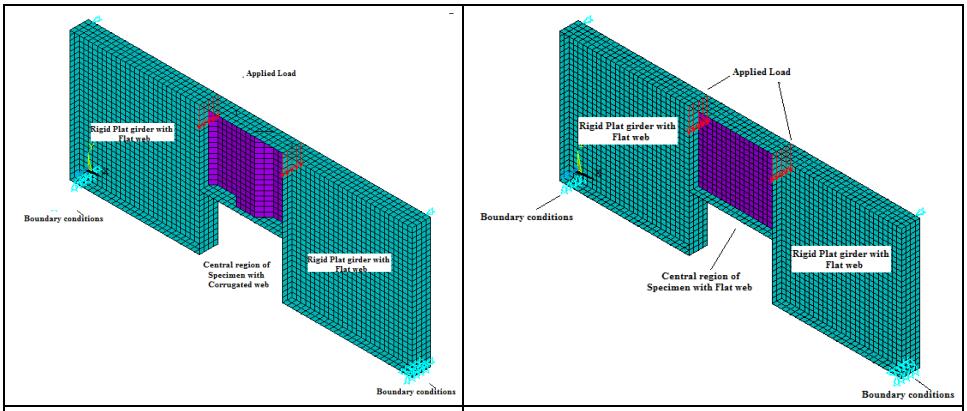

a. CW steel beam model | b. FW steel beam model

Figure 7: Finite element model and boundary conditions

Finite element verifications

Two models were developed to simulate the steel beams with CW or FW under flexural tests for predicting the effect of web shape in flexural capacity of steel beams. This model arrangement with different web configuration was utilized to point out the interaction of bending and web shape. The FE models were verified against experimental results obtained as shown in figures 8 and 9 in terms of vertical displacement verse applied load. These figures show a comparison between the load versus vertical displacement curves obtained from test and from the finite element analysis performed using ANSYS. Fig. 8 shows a comparison between the overall behavior of steel beam with C.W. or F.W. and non-compact flange obtained from tests and that obtained using ANSYS. Fig. 9 shows a similar load versus vertical displacement comparison for steel beams with compact flanges.

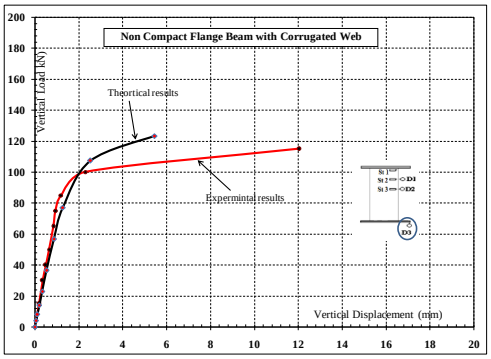

Steel beams with non-compact flanges and CW

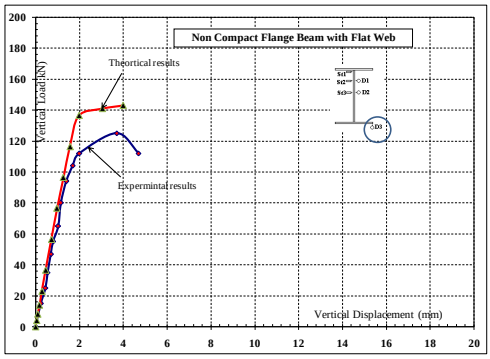

Steel beams with non-compact flanges and FW

Figure 8: comparison between experimental and FEM results

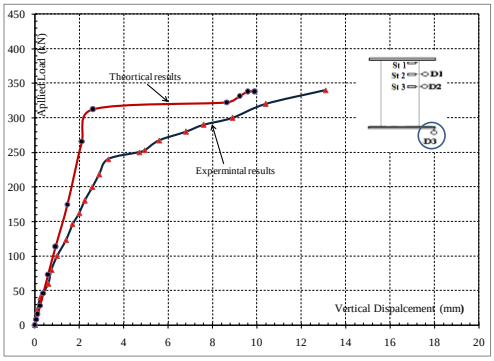

Steel beams with compact flanges and CW

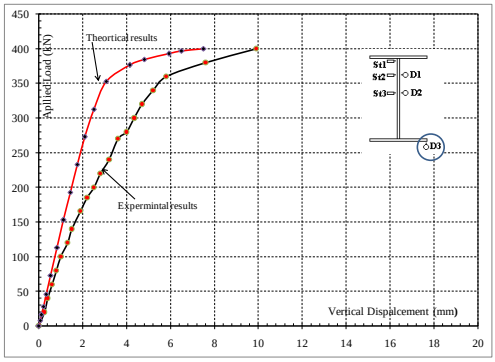

Steel beams with compact flanges and FW

Figure 9: comparison between experimental and FEM results

COMPOSITE CONCRETE/STEEL BEAMS WITH CORRUGATED WEB

Specimens fabrication

The experimental program extended to study this effect when using CW in composite concrete-steel beams. Two composite concrete/steel beams with a corrugated web were fabricated to study the effect of corrugated web on the beam flexural capacity. The concrete slabs and the steel beams were directly connected by shear connectors. Each of the beams was 3100 mm long and simply supported on a span of 3000 mm. The concrete slabs of the composite beams were 900mm long and 500mm wide. Each beam was divided into three lengths; the middle one-third of the span (L=0.9 m) was subjected to a constant moment, wherein both sides of the middle one-third, bare stiffened steel beam were used to prevent shear or moment buckling. The bolted connection between the middle one-third and other parts was designed to ensure failure at a mid-span without slip or bending in the bolts. Figure 10 illustrates the details of fabricated composite beams B1 and B2,which comprised top and bottom steel flanges of 150mm in width and 10mm in thickness, corrugated webs of 130mm in height and 2mm in thickness as well as a top concrete slab. The reinforced concrete slab was 80mm in depth. Meanwhile, the shear connectors had angles measuring 40 × 40 × 4mm with a length of 150mm. The angles were continuously welded to the top steel flange and spaced at 200mm. The concrete slab contained a welded mesh of reinforcement at mid-depth. The mesh reinforcement comprised 10mm diameter high-tensile steel bars that were longitudinally and transversally spaced by 150 mm and 178 mm, respectively. The stiffened and corrugated parts were connected using 10mm thick plates and six M16 grade 10.2 bolts arranged in two columns and three rows. Central distances of 100mm between the columns and 75mm between the rows were used. A seat angle, measuring 100 × 100 × 10mm, was welded at one leg to the bottom steel flange of the tested part and connected with transversal stiffeners by bolts from each end to avoid any failure in the weld between the bottom steel flange and the transversal stiffeners at both ends of the tested part. The component plates and the webs were also accurately machined. The webs in the tested parts were efficiently corrugated to obtain the desired corrugation profiles. Meanwhile, the webs in all beams were continuously welded to the flanges and vertical stiffeners. Beam testing was conducted using a 5000kN-capacity testing machine in the steel construction laboratory of the faculty of engineering at Assiut university; Egypt. The test beams were placed over the support at their ends, which is in line with the end-bearing stiffeners to avoid the local flange and web failure, as shown in Fig. 10. One end of the beams was supported on a roller, and the other on a hinge, to simulate the simply supported condition. The mechanical properties of the flange and the web were the average of the three specimens of the flange and web steel. Table 4 shows the obtained mechanical properties (e.g., modulus of elasticity, elongation percentage, ultimate and yield stresses) for the six tension coupons and average results, respectively. Figure 11 shows load versus vertical displacement curves obtained from tests. Table 5 shows the maximum load and moment achieved by the composite concrete steel beams with corrugated web experimentally.

Table 4: Modulus of Elasticity, Elongation percentage, Ultimate and Yield stresses

Coupon Type	F_Y (N/mm^2)	F_u (N/mm^2)	E (N/mm^2)	δ %
CF	300	375	200000	28
NCF	320	390	213000	25
Web	310	390	205000	24

Table 5: Test results of composite concrete-steel beams

beam No	f_{cu} (N/mm2) N /mm^2	p_{cr} (kN) kN	p_u (kN) kN	P_u / p_{cr}	M_U (KN.m)	Mode of failure
B1	27.5	62	170	2.12	89.25	Flex. Comp. (ductile)
B2	27.5	60	170	2.83	89.25	Flex. Comp. (ductile)

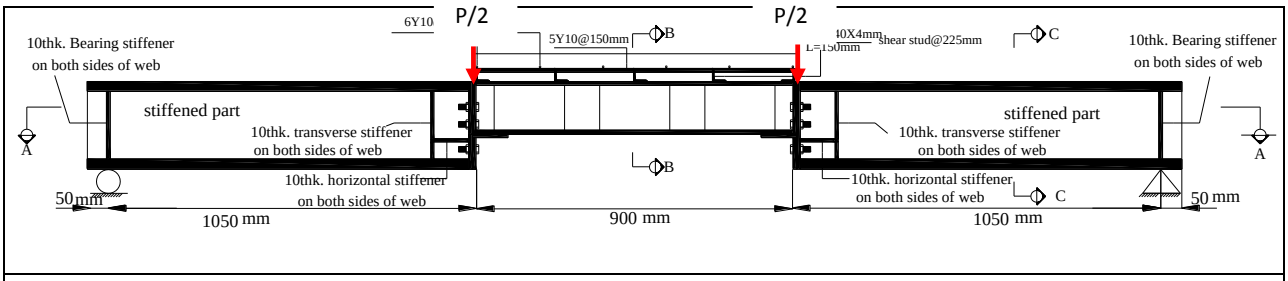

a. Cross-section elevation

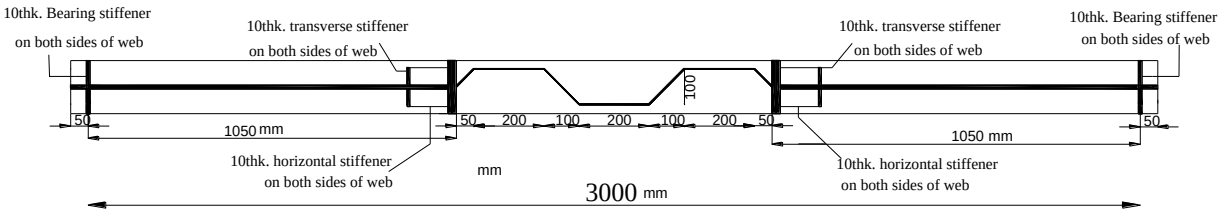

b. Section A-A – Cross-section plan

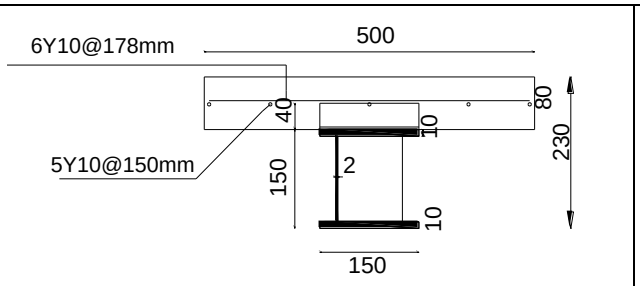

c. Section B-B

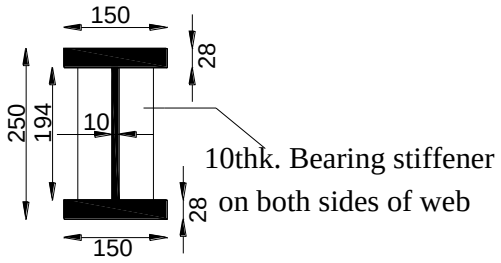

d. Section C-C

Figure 10: Details of test specimens B1 and B2 (all dimensions in mm)

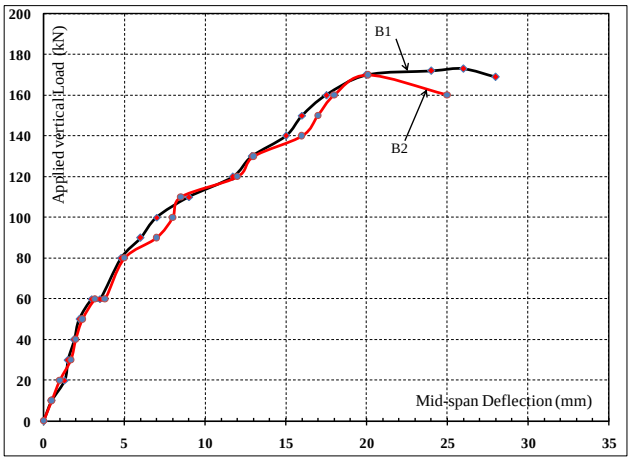

Figure 11: Load–mid-span deflection curve for B1 and B2

Limit state design process

The limit state design is the latest design criteria and procedures given in AS 4100, AS 2327.1, Eurocode 4, AISC-LRFD specifications, and Australian Standards AS/NZS 1170. The limit state design philosophy has been adopted in the current codes of practice as the basic design method for the design of steel and composite structures as it is believed that this method is capable of yielding safer and more economical design solutions. This limit state may be caused by the failure of one or more structural members, the

instability of structural members or the whole structure, or excessive deformations of the structure. In the limit state design, the performance of a structure is evaluated by comparison of design action effects with a number of limiting conditions of usefulness.

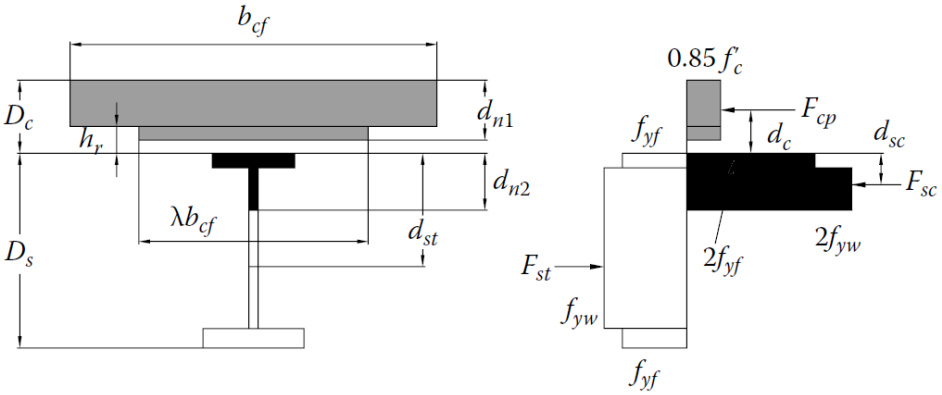

Figure 12: Plastic stress distribution in composite section with $0 \leq \beta \leq 1$.

Using the plastic stress distribution in composite section shown in figure 12 the design equations process will be performed as follow:

The composite beam is designed with (degree of shear connection) $\beta = 0.60$ at the mid-span section as defined in clause 1.4.3 of AS 2327.1 $\left(\beta = \frac{F_{cp}}{F_{cc}}\right)$:

$F_{cc}$is the compressive forces in the concrete slab with complete shear connection

$F_{cp}$is the compressive forces in the concrete slab with partial shear connection

The tensile capacity of the steel section is computed as:

$$F_{st} = \left[(b_{f1} * t_{f1} + b_{f2} * t_{f2}) * f_{yf} + d_w * t_w * f_{yw}\right]$$

The compressive forces in the concrete slab with partial shear connection

$$F_{st} = F_{cc}$$

$$F_{cp} = \beta * F_{cc}$$

The compressive capacity of the concrete slab is computed as:

$$F_{c1} = 0.85 * f'_c * b_{cf} * (D_c - h_r) + A_{s\,bar} * f_{y\,bar}$$

Since $F_{cp}<F_{c1}$, the first plastic natural axis (PNA) lies in the concrete cover slab.

The depth of the first PNA in the concrete slab is calculated as:

$$d_{n1} = \frac{F_{cp}}{0.85 * f'_c * b_{cf}}$$

The compressive force in the steel section is computed as:

$$F_{sc} = F_{st} - F_{cp}$$

The slenderness of the top steel flange in compression is:

$$\lambda_{ef} = \frac{(b_f - t_w) * 0.50}{t_f} * \sqrt{\frac{f_{yf}}{250}}$$

Hence, the top flange of the steel section is compact; the capacity of the steel top flange is:

$$2 * F_{f1} = 2 * b_{f1} * t_{f1} * f_{yf}$$

In this case $F_{sc} < 2 * F_{f1}$, the second natural axis lies in the top flange of the steel section.

The depth of the second neutral axis is computed as:

$$d_{n2} = \frac{F_{sc}}{b_{f1} * (2 * f_{yf})}$$

The distance from the centroid of F_{cp} to top face of the steel section is

$$d_c = D_c - \frac{d_{n1}}{2}$$

The distance from the centroid of F_{st} to the top face of the steel section is given as :

$$d_{st} = \frac{D_s}{2}$$

The distance from the centroid of F_{sc} to the top fiber of the steel section is:

$$d_{sc} = \frac{d_{n2}}{2}$$

The nominal moment capacity is calculated as

$$M_b = F_{cp} * (d_c + d_{sc}) + F_{st} * (d_{st} - d_{sc})$$

The result obtained from the above mentioned design process was the nominal designed moment capacity which found to be equal 84.3 kN.m. This value represents 95% from the maximum moment that the specimens resisted

experimentally. Details of the design process and the final result shown in appendix A of this paper.

CONCLUSIONS

To study the effect of corrugated web on flexural capacity of steel beams, a full scale test was conducted with conventional steel I beams and compared with steel beams with corrugated web. Experimental work has revealed the range where the flexural capacity decreased. The study was extended to compare the nominal moment capacity that can be obtained theoretically from limit state design process and experimentally for composite concrete steel beams with corrugated web. Study results concluded the following:

1- The flexural capacity of steel beam with corrugated web is less than the conventional steel I beam in a range between 10 to 20%.

2- Flexural behavior of steel beam with flat web shows local flange buckling followed by web local buckling, unlike the steel beam with corrugated web which shows earlier flange local buckling only.

3- The flexural capacity of composite concrete-steel beam could be decreased by the same percentages mentioned above in the case of using corrugated web instead of flat web.

4- The finite element model can simulate the behavior of bare steel beams especially in the elastic stage to an acceptable degree of accuracy

REFRENCES

[1] Abbas, H.H., (2003); Analysis and Design of CW Plate Girder for Bridges Using High Performance Steel, Ph.D. Dissertation Lehigh University.

[2] Abbas, H. H., Sause, R., and Driver, R. G. (2006). "Behavior of CW I-girders under in-plane loads." Journal of Engineering Mechanics, ASCE, 132(8), pp.806-814.

[3] Aschinger, R. and Lindner, J. (1997). "Zu Besonderheitenbei Trapezsteg Trägern." Stahlbau, 66(3), pp. 136-142 (in German).

[4] Chan, C. L., Khalid, Y. A., Sahar, B. B., and Hamouda, A.M. S. (2002). "Finite element analysis of corrugated web beams under bending." Journal of Constructional SteelResearch, 58(11), pp. 1391-1406.

[5] Elgaaly, M., Seshadri, A., and Hamilton, R. W. (1997)."Bending strength of steel beams with CWs." Journal of Structural Engineering, ASCE, 123(6), pp.772-782.

[6] Huang, L., Hikosaka, H., and Komine, K. (2004)."Simulation of accordion effect in corrugated steel web with concrete flanges." Computers and Structures, 82, pp.2061-2069.

[7] Johnson, R. P. and Cafolla, J. (1997). "Local flange bucklingin plate girders with corrugated steel webs." Proc.Institution of Civil Engineers-Structures and Buildings,122(2), pp. 148-156.

[8] Khalid, Y. A., Chan, C. L., Sahari, B. B., and Hamouda, A.M. S. (2004). "Bending behaviour of corrugated web beams." Journal of Materials Processing Technology,150(3), pp. 242-254.

[9] Leiva-Aravena, L. (1987). Trapezoidally Corrug-ated Panels: Buckling Behaviour under Axial Compressionand Shear. Publication S: 87(1), Division of Steel andTimber Structures, Chalmers University of Technology,Gothenburg, Sweden.

[10] Lindner, J. (1992). "Zur Bemessung von Trapezsteg Trägern." Stahlbau, 61(10), pp. 311-318 (in German).

[11] Metwally, A. E. and Loov, R. E. (2003). "Corrugated steel webs for prestressed concrete girders." Materials and Structures, 36(2), pp. 127-134.

[12] Oh, J. Y., Lee, D. H., and Kim, K. S. (2012). "Accordion effect of prestressed steel beams with CWs." Thin-Walled Structures, 57, pp. 49-61.

[13] Pasternak and Kubieniec, (2010), "Plate girders with corrugated webs" Journal of Civil Engineering and Management, 16(2), pp. 166-171

[14] Protte, W. (1993). "Zur Gurtbeulungeines Trägernmit Profiliertem Stegblech." Stahlbau, 62(11), pp. 327-332 (in German).

[15] Sayed-Ahmed, E. Y. (2007). "Design aspects of steel I girders with corrugated steel webs." Electronic Journal of Structural Engineering, 7, pp. 27-40.

[16] Watanabe, K. and Kubo, M. (2006). "In-plane bending capacity of steel girders with corrugated web plates." Journal of Japan Society of Civil Engineers, 62(2), pp. 323-336 (in Japanese).

Nomenclature

b : The length of the horizontal panel
b_f : Flange width
c : Distance between flange plastic hinges
d : projected length of the inclined panel
d_c : The distance from the centroid of F_{cp} to top face of the steel section
d_{st} : The distance from the centroid of F_{st} to the top face of the steel section
d_{sc} : The distance from the centroid of F_{sc} to the top fiber of the steel section
E: : Modulus of elasticity
F_{f1} : Capacity of the steel top flange
F_{cc} : is the compressive forces in the concrete slab with complete shear connection
F_{cp} : is the compressive forces in the concrete slab with partial shear connection
F_{sc} : The compressive force in the steel section
f_{cu} : Concrete compressive strength
f_{yf} : Flange yield stress
f_{yw} : Web yield stress
h_r : The corrugation depth
M_b : The nominal moment capacity
M_d : The design nominal moment capacity
P_u : Ultimate load achieved experimentally.
t_w : Web thickness
t_f : Flange thickness
θ : The corrugation angle
β : Degree of shear connection
λ_{ef} : The slenderness of the top steel flange in compression

Appendix A

The composite beam is designed with (degree of shear connection) β = 0.60 at the mid-span section as defined in clause 1.4.3 of AS 2327.1 $\left(\beta = \frac{F_{cp}}{F_{cc}}\right)$:

$F_{cc}$is the compressive forces in the concrete slab with complete shear connection

$F_{cp}$is the compressive forces in the concrete slab with partial shear connection

The tensile capacity of the steel section is computed as:

$$F_{st} = \left[\left(b_{f1} * t_{f1} + b_{f2} * t_{f2}\right) * f_{yf} + d_w * t_w * f_{yw}\right] * 0.85$$

$$F_{st} = [(150 * 10 + 150 * 10) * 310 + 130 * 2 * 310] * 0.85 \quad = 859010\ N$$

The compressive forces in the concrete slab with partial shear connection

$$F_{st} = F_{cc}$$

$$F_{cp} = \beta * F_{cc}$$

$$F_{cp} = 0.6 * 859.01 \quad = 515.406\ \text{kN}$$

The compressive capacity of the concrete slab is computed as:

$$F_{c1} = 0.85 * f_c' * b_{cf} * (D_c - h_r) + A_{s\,bar} * f_{y\,bar}$$

$$F_{c1} = 0.85 * 27.5 * 500 * (80) + 5 * 78.57 * 360 = 1076429\ N \quad = 1076.43kN$$

Since F_{cp}<F_{c1}, the first plastic natural axis (PNA) lies in the concrete cover slab.

The depth of the first PNA in the concrete slab is calculated as:

$$d_{n1} = \frac{F_{cp}}{0.85 * f_c' * b_{cf}}$$

$$d_{n1} = \frac{515.406 * 1000}{0.85 * 27.5 * 500} = 44.1\ mm$$

The compressive force in the steel section is computed as:

$$F_{sc} = F_{st} - F_{cp}$$

$$F_{sc} = 859.01 - 515.406 = 343.6\ kN$$

The slenderness of the top steel flange in compression is:

$$\lambda_{ef} = \frac{(b_f - t_w) * 0.50}{t_f} * \sqrt{\frac{f_{yf}}{250}}$$

$$\lambda_{ef} = \frac{(150 - 2) * 0.50}{10} * \sqrt{\frac{310}{250}} = 8.2 < 9$$

Hence, the top flange of the steel section is compact; the capacity of the steel top flange is:

$$2 * F_{f1} = 2 * b_{f1} * t_{f1} * f_{yf}$$

$$2 * F_{f1} = 2 * 150 * 10 * 310 \quad = 930000N = 930\ kN$$

If $F_{sc} < 2 * F_{f1}$, the second natural axis lies in the top flange of the steel section.

The depth of the second neutral axis is computed as:

$$d_{n2} = \frac{F_{sc}}{b_{f1} * (2 * f_{yf})}$$

$$d_{n2} = \frac{343.06 * 1000}{150 * (2 * 310)} = 3.69\ mm < t_f$$

The distance from the centroid of F_{cp} to top face of the steel section is

$$d_c = D_c - \frac{d_{n1}}{2}$$

$$d_c = 80 - \frac{44.1}{2} = 58\ mm$$

The distance from the centroid of F_{st} to the top face of the steel section is given as :

$$d_{st} = \frac{D_s}{2}$$

$$d_{st} = \frac{150}{2} = 75\ mm$$

The distance from the centroid of F_{sc} to the top fiber of the steel section is:

$$d_{sc} = \frac{d_{n2}}{2}$$

$$d_{sc} = \frac{3.69}{2} = 1.8\ mm$$

The nominal moment capacity is calculated as

$$M_b = F_{cp} * (d_c + d_{sc}) + F_{st} * (d_{st} - d_{sc})$$

$$M_b = 515406 * (58 + 1.8) + 859010 * (75 - 1.8) = 93700000 \quad = 93.7\ kN.m$$

$$M_d = \phi * M_b = 0.9 * 93.7 = 84.3\ kN.m$$